

Evidence of a rhodium catalytic species containing a bridging 1,2-diphosphine in styrene hydroformylation

Zoraida Freixa,^a Mariette M. Pereira,^a Alberto A. C. C. Pais^b and J. Carles Bayón^{*a}

^a *Departament de Química, Universitat Autònoma de Barcelona, Bellaterra, 08193 Barcelona, Spain*

^b *Departamento de Química, Universidade de Coimbra, Rua Larga, 3049 Coimbra, Portugal*

Received 19th May 1999, Accepted 23rd July 1999

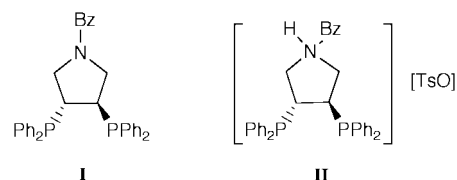
A systematic analysis of the effect of pressure, temperature and ligand : metal molar ratio on the selectivity of styrene hydroformylation catalysed by rhodium and (3*R*,4*R*)-1-benzyl-3,4-bis(diphenylphosphino)pyrrolidine ligand **I** was carried out. The enantioselective discrimination was insignificant in all cases and the regioselectivity nearly identical to that obtained with the Rh–PEtPh₂ catalyst under the same reaction conditions. An NMR study was performed in order to elucidate the species formed in both systems under catalytic reaction conditions. Molecular mechanics calculations were also carried out in an attempt to rationalize the catalytic and NMR experiments. Thus, evidence is provided for bridging co-ordination of the diphosphine **I** in different rhodium complexes. The presence of these species in the hydroformylation reaction accounts for the selectivity observed. The results for this catalytic system were compared with those for related diphosphines already reported.

Introduction

Hydroformylation is one of the most important processes among those using homogeneous transition metal catalysts. The synthesis of optically active aldehydes from easily available olefins is an attractive strategy for the production of useful building blocks in the synthesis of biologically active products. Thus, in the last twenty years, great effort has been made in the design of enantioselective hydroformylation catalysts. Until the beginning of this decade, Pt–Sn catalysts with selected chiral diphosphines gave the best enantiomeric excesses (e.e.), although chemo- and regio-selectivities obtained with these systems were often not satisfactory.¹ However, in recent years, remarkable results have been reported in the area of asymmetric rhodium catalysed hydroformylation.² Phosphine–phosphite,³ diphosphite⁴ and diphosphinite⁵ co-catalyst ligands have provided excellent chemo- and regio-selectivities, as well as 60 to 95% e.e., mainly in the hydroformylation of vinylarenes. The phosphine–phosphite ligand BINAPHOS (BINAPHOS = (*R*)-[2-(diphenylphosphino)-1,1'-binaphthalen-2'-yl]-[(*S*)-1,1'-binaphthalen-2,2'-yl]phosphite) has also been successfully applied to other types of substrates.⁶ In spite of the amount of work accumulated, it is not clear what the crucial factors in the design of ligands for highly enantioselective rhodium catalysts are. For instance, BINAPHOS and the diphosphinite ligands have C₁ symmetry, while the diphosphites have C₂ symmetry. Furthermore, BINAPHOS adopts an axial–equatorial co-ordination in the putative rhodium trigonal bipyramidal species [RhH(PP)(CO)₂] (PP = diphosphine ligand) under syn-gas (CO + H₂), while the diphosphites form equatorial–equatorial species. Nevertheless, a common characteristic of all these highly enantioselective systems is that they do not form classical five or six membered chelating rings, which are common in catalytic species used in other asymmetric reactions. Finally, the best performing enantioselective catalysts for hydroformylation also seem to form a single active catalytic species, as shown in some cases by spectroscopic techniques.⁷

Recently, in the hydroformylation of styrene with a rhodium catalyst modified with 2,4-bis(diphenylphosphino)pentane (bdpp), a significant enhancement in the regio- and enantioselectivity has been reported with increase of the ligand to metal molar ratio.⁸ In this case, high pressure NMR and IR

revealed that, under syn-gas, the axial–equatorial co-ordinated complex [RhH(PP)(CO)₂] (PP = bdpp) is the only active species, which is in equilibrium with the inactive dimer [Rh₂(PP)₂(CO)₄].⁹ Interestingly, when 2,3-bis(diphenylphosphino)butane (chiraphos) was used in the same reaction instead of bdpp, increase in the ligand to metal molar ratio produces a drop in the enantioselectivity of the reactions.¹⁰ These unexpected results prompted us to study the hydroformylation of styrene catalysed by rhodium and the ligand (3*R*,4*R*)-1-benzyl-3,4-bis(diphenylphosphino)pyrrolidine **I**. This 1,2-diphosphine was first reported by Nagel *et al.*¹¹ and it should form a more strained chelate ring than chiraphos. On the other hand, the pyrrolidinic backbone should produce a wider P–Rh–P chelate angle, thus resembling that of ligand bdpp. In this paper we describe the effects of the ligand : metal molar ratio and the reaction conditions (temperature and pressure) on the selectivity of the hydroformylation of styrene catalysed by rhodium and ligand **I**. The results are compared with those of the Rh–PEtPh₂ catalyst. We also present NMR and molecular mechanics studies in an attempt to explain the differences observed between this and structurally related catalytic systems.



Results and discussion

Catalytic results

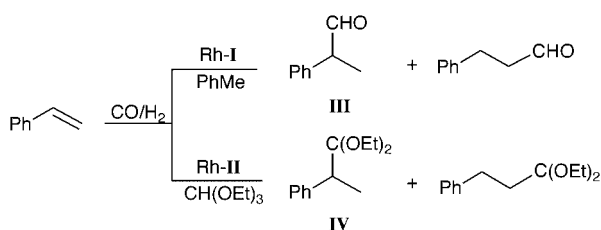
The rhodium diphosphine catalyst was generated by mixing appropriate amounts of [Rh₂(μ-OMe)₂(cod)₂] and compound **I** under CO and H₂ pressure. Styrene was used as substrate to test the activity and selectivity of the catalysts in the hydroformylation reaction (Scheme 1).

Table 1 lists the results of the reaction at 80 and 65 °C, in a pressure range from 8 to 30 bar, and diphosphine : metal molar ratio between 1.25 and 2 : 1. In all the experiments, samples were

Table 1 Hydroformylation of styrene with rhodium catalyst and ligand **I** and PEtPh_2

Entry	$T/^\circ\text{C}$	P/bar	I :Rh ^a	PEtPh_2 :Rh ^a	t/h	% Conversion ^b	% Aldehyde ^c	% Branched aldehyde ^d	% e.e. ^e
1	65	8	1.25	0	6	53	>99	86	<2
2	65	8	2	0	22	97	99	94	<2
3	65	30	1.25	0	8	72	99	90	3
4	65	30	2	0	8	91	98	86	<2
5 ^f	65	30	2	0	8	49	>99	87	4
6	80	8	1.25	0	11	97	>99	69	4
7	80	8	2	0	12	90	>99	86	3
8	80	30	1.25	0	7	98	99	88	<2
9	80	30	2	0	7	99	98	84	4
10	65	8	0	2	2	97	>99	85	—
11	65	30	0	2	1.4	98	>99	90	—
12	80	8	0	2	0.4	87	>99	68	—

^a Ligand to metal molar ratio. ^b Converted olefin as percentage of the initial amount. ^c Percentage of aldehydes relative to the olefin converted. ^d Branched aldehyde **III** relative to the total amount of aldehyde formed. ^e Enantiomeric excess of the *S* isomer. Reaction conditions: 10 mmol of styrene, 0.0125 mmol of $[\text{Rh}_2(\mu\text{-OME})_2(\text{cod})_2]$, and the appropriate amount of **I** or PEtPh_2 in 15 ml of toluene; $P(\text{CO}) = P(\text{H}_2)$. ^f Reaction was run with the cationic diphosphine **II** in $\text{CH}(\text{OEt})_3$, and the corresponding ethyl acetals were obtained (see text).



taken from the autoclave during the reaction and the composition of the mixture was analysed. The results showed that both the regio- and enantio-selectivity were constant throughout time within the experimental error range ($\pm 1\%$), which indicates that the catalytically active species did not significantly evolve during the process.

As expected, the rhodium–diphosphine catalyst is highly chemoselective, since ethylbenzene was always less than 2%. The enantiomeric excess found for 2-phenylpropanal **III** was insignificant ($\leq 6\%$), regardless of the reaction conditions employed. Therefore, contrary to the case of *bdpp* or *chiraphos*, no effect was observed on the stereoselectivity by changing the metal to ligand molar ratio. Since the enantiomeric excess did not depend on the conversion, the low stereoselectivity could not be attributed to a racemization of the aldehyde. However, since the amine group of the diphosphine ligand could catalyse the enolization of the aldehyde, an experiment was designed to discard epimerization of **III**. Direct synthesis of ethyl acetals under hydroformylation conditions can minimize aldehyde racemization. In the case of platinum–phosphine hydroformylation catalysts this is achieved by using triethyl orthoformate as a solvent, the metal complex acting as catalyst for the transacetalization reaction.¹² However, when rhodium–phosphine catalysts are used an additional acid catalyst is required to form the acetals. Pyridinium *p*-toluenesulfonate has been reported efficiently to catalyse the acetalization of aldehydes formed under hydroformylation conditions.¹³ Following this approach, we have used the ammonium tosylate salt **II** as acid catalyst. This was synthesized by mixing ether solutions of ligand **I** with *p*-toluenesulfonic acid. Using triethyl orthoformate as solvent and **II** as co-catalyst (entry 5), at 65 °C and 30 bar, a 4% e.e. was obtained, which is nearly identical to the value found with co-catalyst **I** in toluene under the same reaction conditions (entry 4). Although the reaction rate in $\text{HC}(\text{OEt})_3$ is significantly slower, the same regioselectivity (87%) was observed in the two experiments for the branched acetal **IV** and aldehyde **III**. Thus, protonation of the pyrrolidine does not affect the intrinsic selectivity of the

catalyst, but efficiently catalyses the *in situ* acetalization of the aldehydes. The conclusion is that the enolization of aldehyde **III** is not responsible for the very low e.e. obtained with the rhodium/ligand **I** catalytic system.

At all the pressures and temperatures tested, the regioselectivity in the branched aldehyde **III** depends on the ligand: metal molar ratio. The effect is, however, more remarkable at low pressures. Rhodium catalysts containing diphosphines *bdpp* and *chiraphos* showed an increase of the regioselectivity in the branched aldehyde **III** when the pressure is raised or the temperature is decreased, regardless of the ligand: metal molar ratio used.¹⁰ In the case of the catalytic system Rh/ligand **I**, the selectivity in the branched aldehyde at $[\text{I}]/[\text{Rh}] = 1.25$ follows the same trend observed for *chiraphos* and *bdpp* (entries 1, 3, 6 and 8). At ligand: metal molar ratio = 2:1 a drop in the selectivity was observed when the pressure was raised (entries 2, 4 and 7, 9). These results suggest some differences between the catalytic system formed with ligand **I** and those of *bdpp* or *chiraphos*.

The hydroformylation of styrene catalysed by rhodium and the phosphine PEtPh_2 was also studied and compared with the results obtained with ligand **I**. Ethyldiphenylphosphine was chosen to simulate the electronic and steric properties of the diphosphine **I** co-ordinating as a monodentate ligand. The most significant feature observed is the nearly identical selectivity achieved at $[\text{I}]/[\text{Rh}] = 1.25$ and $[\text{PEtPh}_2]/[\text{Rh}] = 2$ (entries 1, 10; 3, 11; 6, 12). Furthermore, the rate observed for the monophosphine catalyst was 4–10 times higher than that for the diphosphine **I**. These results could be explained by considering that the latter forms a rhodium species where the ligand is co-ordinated in monodentate mode. The rhodium species could be the fastest catalyst among the other active species in the reaction mixture. Therefore, even if it is present at low concentration, most of the converted olefin would circulate through this active species, which is structurally related to the catalyst formed by Rh with PEtPh_2 . Both the similar regioselectivity obtained with ligand **I** and PEtPh_2 and the very low e.e. reached with the former can be rationalized in this way. To summarize, ligand **I** shows a different catalytic behaviour to that of *bdpp* or *chiraphos* since it renders very low e.e. under all the reaction conditions tested. Furthermore, the regioselectivities obtained are nearly identical to those measured in experiments with PEtPh_2 at a similar P:Rh molar ratio.

NMR experiments

Since the catalytic results suggest the presence of species in which there is only one phosphorus atom of ligand **I** per rhodium atom, *i.e.* monodentate or bridging bidentate co-

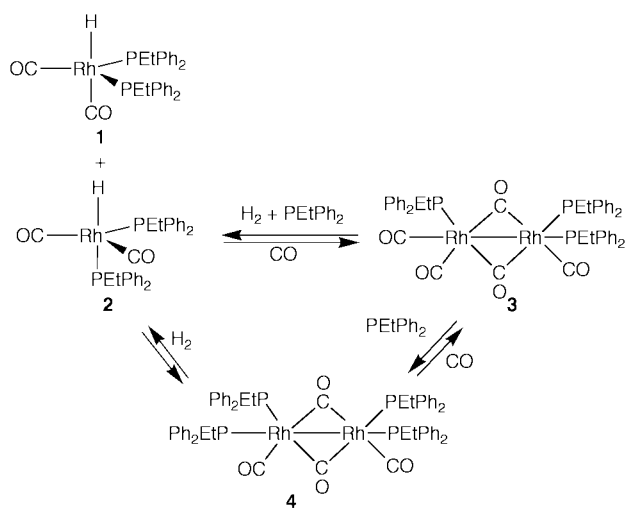
Table 2 The $^{31}\text{P}\{-^1\text{H}\}$ and ^1H NMR data for the species of the Rh-PETPh₂ catalytic system under 30 bar of CO/H₂ (1:1)^a

Species	^{31}P δ , J/Hz	^1H δ , J/Hz
1 and 2 ^b	31.2 (d); $J_{\text{Rh-P}} = 131$	-9.3 (td); $J_{\text{P-H}} = 15$, $J_{\text{Rh-H}} = 7$
3 ^b	20.3 ^c (dt); $^1J_{\text{Rh-P}} = 135$, $^3J_{\text{P-P}} = 12$, $^2J_{\text{Rh-P}} < 2$, 16.4 ^d (ddd); $^1J_{\text{Rh-P}} = 152$, $^3J_{\text{P-P}} = 12$, $^2J_{\text{Rh-P}} = 8$	
4 ^d	14.0 (br d); $^1J_{\text{Rh-P}} = 147$	

^a d = doublet; td = triplet of doublets; dt = doublet of triplets; ddd = doublet of doublets of doublets; br = broad. ^b Observed at PETPh₂:Rh molar ratios 2 and 4:1. ^c The signals at δ 16.4 and 20.3 integrate 2:1. ^d Observed at PETPh₂:Rh molar ratio 4:1.

ordination, an NMR study was undertaken to provide some direct experimental evidence of this unusual co-ordination for a 1,2-diphosphine.

First, we analysed the species formed in mixtures of [Rh₂(μ -OMe)₂(cod)₂] and PETPh₂ under CO and H₂ pressure (30 bar), as a model system for the monodentate co-ordination of ligand **I**. The data are collected in Table 2. When the phosphine:metal molar ratio is 2:1, the $^{31}\text{P}\{-^1\text{H}\}$ NMR shows a doublet centred at δ 31.2 ($J_{\text{Rh-P}} = 131$ Hz), which is associated with a hydride signal split into a triplet of doublets (δ -9.3; $J_{\text{P-H}} = 15$, $J_{\text{Rh-H}} = 7$ Hz). No other hydride signals are observed in this system. This small P-H coupling constant is characteristic of phosphines co-ordinated in equatorial positions of a trigonal bipyramidal complex. However, a recent report¹⁴ suggests that a $J_{\text{P-H}} = 15$ Hz could correspond to a mixture of axial-equatorial and equatorial-equatorial isomers in fast equilibrium, roughly in 1 to 3 molar ratio. Thus, species [RhH(CO)₂(PETPh₂)₂] **1** and **2** in Scheme 2 must be responsible for these ^{31}P



and ^1H NMR signals. The complex [RhH(CO)₂(PPh₃)₂] is also known to exist in a mixture of equatorial-equatorial and axial-equatorial (85:15) isomers.¹⁵

At a molar ratio PETPh₂:Rh = 2:1 the $^{31}\text{P}\{-^1\text{H}\}$ NMR shows two additional signals centred at δ 16.4 and 20.3, the first being twice as intense as the second. The pattern of these signals can be satisfactorily simulated (Fig. 1) with the parameters in Table 2 for the binuclear species **3** (Scheme 2). When the phosphine to rhodium molar ratio was increased to 4:1 the signals of the mononuclear and binuclear species broadened, and a new broad and weak doublet centred at δ 14.0 ($J_{\text{Rh-P}} = 147$ Hz) appeared. This could correspond to a species **4** (Scheme 2), structurally related to **3**. In fact, both the ^{31}P NMR chemical shift and the $J_{\text{Rh-P}}$ of **4** are very similar to those of the com-

Table 3 The $^{31}\text{P}\{-^1\text{H}\}$ and ^1H NMR data for species formed in solutions of the reaction between [RhH(CO)(PPh₃)₃] **5** and ligand **I**^a

Species	^{31}P δ , J/Hz	^1H δ , J/Hz
5	42.5 (d); $J_{\text{Rh-P}} = 151$	-9.7 (br s) ^b
6 ^c	45.4 (ddd); $J_{\text{Rh-P}} = 134$, $J_{\text{P-P}} = 73$, 30	-10.5 (dddd); $J_{\text{P-ax-H}} = 74$, $J_{\text{P-eq-H}} = 28$, $J_{\text{P-eq-H}} = 18$
	41.3 (ddd); $J_{\text{Rh-P}} = 119$, $J_{\text{P-P}} = 30$, 16	$J_{\text{Rh-H}} = 9$
	38.1 (ddd); $J_{\text{Rh-P}} = 142$, $J_{\text{P-P}} = 73$, 16	-11.6 (qd); $J_{\text{P-H}} = 17$, $J_{\text{Rh-H}} = 9$
7 ^d	41.0 (d); $J_{\text{Rh-P}} = 145$	

^a s = singlet; qd = quintuplet of doublets; dddd = doublet of doublets of doublets of doublets. ^b Observed as a quadruplet ($J_{\text{P-H}} = 13$ Hz) at -50 °C. ^c Observed in solutions with molar ratios **I**:**5** \leq 1:1. ^d Observed in solutions with molar ratios **I**:**5** = 2:1.

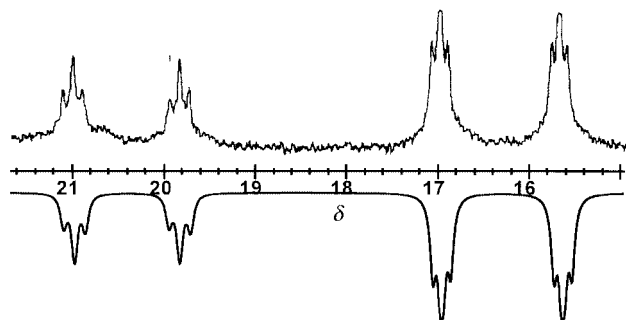


Fig. 1 The $^{31}\text{P}\{-^1\text{H}\}$ NMR spectrum of species **3**. Top: experimental. Bottom: simulated with constants in Table 2.

parable phosphorus in species **3**. However, the lack of a fine structure in the NMR signal does not allow an unequivocal assignment for species **4**.

In a second set of experiments the reaction between [RhH(CO)(PPh₃)₃] **5** and ligand **I** was studied by NMR at different molar ratios. The results are collected in Table 3. It is worth noting that these reactions produced a complex system with different species, even at low ligand to complex molar ratio, in contrast with the reported results of reaction of **5** and classical chelating diphosphanes, which yields a single species [RhH(CO)(PP)(PPh₃)₂] (PP = diphosphane).^{16,17}

When the molar ratio **I**:**5** \leq 1:1 the hydride region of the ^1H NMR shows a broad signal centred at δ -9.7, which sharpens at +60 °C, and becomes the characteristic broad quadruplet ($J_{\text{P-H}} = 13$ Hz) of [RhH(CO)(PPh₃)₃] at -50 °C.¹⁵ The characteristic signal for this compound was also observed in the $^{31}\text{P}\{-^1\text{H}\}$ NMR.¹⁷

At a molar ratio **I**:**5** \leq 1 a 14-line signal, centred at δ -10.5 (Fig. 2a) was also observed in the ^1H NMR spectrum. This signal could correspond to a five-co-ordinated species [RhH(CO)(PP)(PPh₃)₂] where PP is ligand **I** co-ordinating at axial and equatorial positions. Consistently, this species occurs as a 24 line-signal in the $^{31}\text{P}\{-^1\text{H}\}$ NMR spectrum corresponding to the three chemically different P atoms, as is shown in Fig. 3. However, the chemical shifts for the phosphorus of the diphosphine (δ 41.3 and 38.1) are unexpectedly low for a five member chelate ring (see below),¹⁸ but they are closer to those observed for the five-co-ordinate species with PETPh₂. Thus, a binuclear structure [Rh₂H₂(CO)₂(PP)₂(PPh₃)₂] **6** in Scheme 3, with two bridging diphosphines is proposed for this complex.

When the molar ratio **I**:**5** was raised to 2:1 a new doublet (δ 41.0; $J_{\text{Rh-P}} = 145$ Hz) occurs in the $^{31}\text{P}\{-^1\text{H}\}$ NMR, which is associated with a hydride signal centred at δ -11.6. The last is split into a quintuplet of doublets, as shown in Fig. 2b. Similar coupling constants, for both ^{31}P and ^1H , have been reported for species [RhH(PP)₂] (PP = 1,2- or 1,3-diphosphines) with a fluxional distorted trigonal bipyramidal geometry, which renders the four phosphorus atoms equivalent in solution.^{9,19} Again, in

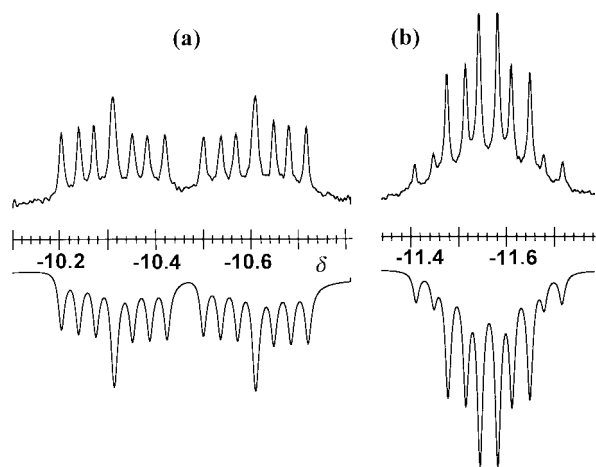


Fig. 2 (a) Top, hydride signal of the ^1H NMR spectrum of species **6**; bottom, simulated spectrum with constants in Table 3. (b) Top, hydride signal of the ^1H NMR spectrum of species **7**; bottom, simulated spectrum with constants in Table 3.

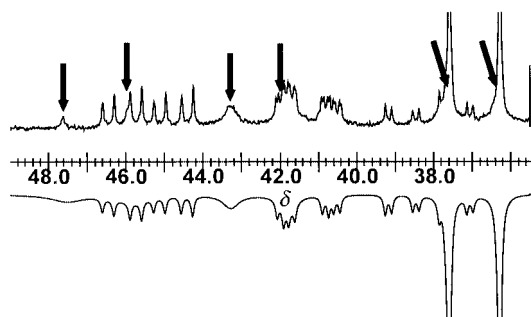
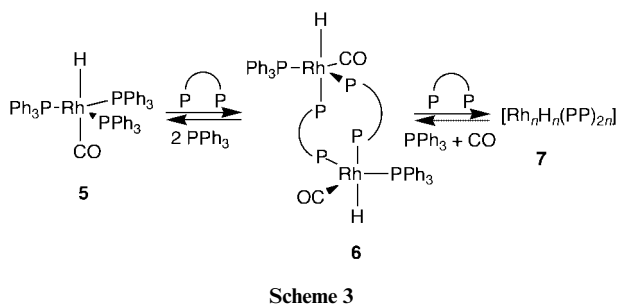


Fig. 3 The $^{31}\text{P}\{-^1\text{H}\}$ NMR spectrum of species **6**. Top: experimental. Bottom: simulated with constants in Table 3. The arrows indicate signals corresponding to other species, which were also added to the simulation.



this case the phosphorus signal of the complex with ligand **I** shows a chemical shift too low for a five membered chelated ring. For instance, the complex with 1,2-bis(diphenylphosphino)ethane (dppe) shows δ 57.²⁰ Thus, we conclude that in the complex with ligand **I** the diphosphine must be co-ordinated to two different rhodium atoms, forming an oligomeric species $[\text{Rh}_n\text{H}_n(\text{PP})_{2n}]$ **7**. It was not possible to determine the precise nature of this complex, but an inspection of the molecular models shows that a binuclear structure with four bridging diphosphines is probably too sterically hindered.

In addition to the signals of species **5**–**7** two other doublets were observed in $^{31}\text{P}\{-^1\text{H}\}$ NMR spectra of the reactions of **5** with ligand **I**. These signals could not be assigned. The first doublet (δ 46.7; $J_{\text{Rh-P}} = 167$ Hz) appears in solutions with molar ratios **I**:**5** = 0.5:1, the second (δ 37.0; $J_{\text{Rh-P}} = 132$ Hz) at molar ratios between 0.5 and 2:1. The intensity of the first doublet decreased when PPh_3 was added to solutions with molar ratio = 0.5:1, while that of the second significantly increased. At these molar ratios both dppe²¹ and dppp ($\text{Ph}_2\text{PCH}_2\text{CH}_2\text{CH}_2\text{PPh}_2$)¹⁷

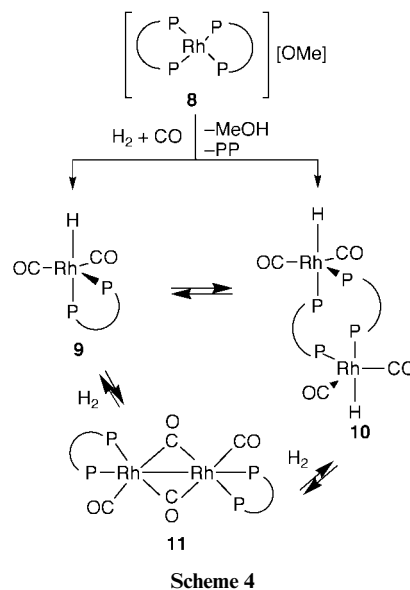
Table 4 The $^{31}\text{P}\{-^1\text{H}\}$ and ^1H NMR data for species of the rhodium–ligand **I** catalytic system under 30 bar of CO-H_2 (1:1)

Species	^{31}P δ , J/Hz	^1H δ , J/Hz
8	60.5 (d); $J_{\text{Rh-P}} = 133$	
9	69.8 (d); $J_{\text{Rh-P}} = 116$	–8.2 (td); $J_{\text{P-H}} = 61$, $J_{\text{Rh-H}} = 12$
10	40.6 (d); $J_{\text{Rh-P}} = 115$	–9.3 (td); $J_{\text{P-H}} = 62$, $J_{\text{Rh-H}} = 10$
11^a	46.3 (br d); $J_{\text{Rh-P}} = 147$	
	42.1 (br d); $J_{\text{Rh-P}} = 129$	
12^b	23.6 (d); $J_{\text{Rh-P}} = 139$	
	25.3 (d); $J_{\text{Rh-P}} = 119$	

^a Registered at 65 °C; it occurs as a doublet (δ 45.3, $J_{\text{Rh-P}} = 130$ Hz) at room temperature. ^b Registered at 65 °C.

form uncharacterized species with nearly identical P–Rh coupling constants to those observed with ligand **I**. However, the chemical shifts observed for dppe and dppp are characteristic of chelated ligands.

Finally, the system rhodium–ligand **I**, under CO and H_2 pressure, was analysed by NMR. Thus, the complex $[\text{Rh}_2(\mu\text{-OMe})_2(\text{cod})_2]$ and **I** (1:1.25) in d_8 -toluene was pressurized with 30 bar of syn-gas. The data are summarized in Table 4. First, a doublet at δ 60.5 ($J_{\text{Rh-P}} = 133$ Hz) was observed in the $^{31}\text{P}\{-^1\text{H}\}$ NMR. This is assigned to a species **8** in Scheme 4, by comparison with



the homologous cationic complex with dppe (δ 57; $J_{\text{Rh-P}} = 133$ Hz).²⁰ Species **8** slowly evolves under syn-gas to form the neutral hydrido species described below. A cationic species with the same structure is reported to form by reaction of $[\text{Rh}_2(\mu\text{-OMe})_2(\text{cod})_2]$ and bdpp. This also evolves to hydrido carbonyl complexes under syn-gas.⁹

The ^1H NMR (Fig. 4) shows two very similar triplets of doublets (δ –8.2, $J_{\text{P-H}} = 61$, $J_{\text{Rh-H}} = 12$ Hz; δ –9.3, $J_{\text{P-H}} = 62$, $J_{\text{Rh-H}} = 10$ Hz) characteristic of trigonal pyramidal $[\text{RhH}(\text{CO})_2(\text{PP})]$ species, where the diphosphine (PP) is co-ordinated in axial–equatorial positions and the phosphorus atoms are involved in a fast exchange process.⁹ These signals remain invariable down to –40 °C. Selective decoupling experiments show that the signal centred at δ –8.2 is associated with a doublet at δ 69.8 ($J_{\text{Rh-P}} = 116$ Hz) in the $^{31}\text{P}\{-^1\text{H}\}$ NMR spectrum. The coupling constant is an average value for phosphorus co-ordinated in equatorial and axial positions and the chemical shift is characteristic of a five-membered chelated diphosphine. Thus, these signals correspond to classical species **9** in Scheme 4. Very similar coupling constants were reported for $[\text{RhH}(\text{CO})_2(\text{PP})]$ (PP = bdpp), for which the same structure is proposed.⁹ However, as expected for a five-membered chelate

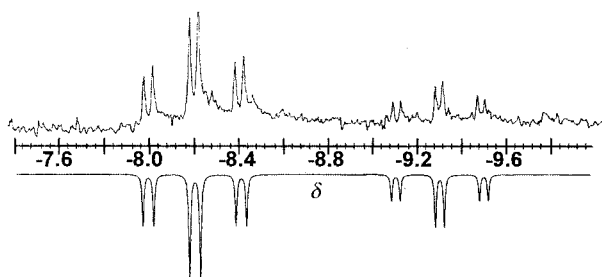


Fig. 4 Hydride signal in the ^1H NMR spectra of species **9** and **10**. Top: experimental spectrum. Bottom: simulated with constants in Table 4.

ring, the doublet of **9** in the $^{31}\text{P}\{-^1\text{H}\}$ NMR is shifted to lower fields.¹⁸

Since the second hydride signal centred at $\delta -9.3$ displays a nearly identical pattern, a closely related structure to that of complex **9** must be responsible for the second triplet of doublets in the ^1H NMR. Selective decoupling experiments allow the last signal to be associated with the $^{31}\text{P}\{-^1\text{H}\}$ NMR doublet at $\delta 40.6$ ($J_{\text{Rh-P}} = 115$ Hz). The value of the Rh–P coupling constant, almost equal to that of **9**, corroborates the equatorial–axial co-ordination of the phosphorus atoms in this species. However, the chemical shift is characteristic of monodentate co-ordinated phosphines, as was shown in the experiments with PEtPh_2 described before. These results are consistent with a binuclear species **10** in Scheme 4, where the diphosphine is bridging two rhodium atoms, although a structure with higher nuclearity cannot be totally discarded. As expected, the signals corresponding to **10** decrease with respect to those of the mononuclear species **9** when the temperature is raised.

The other two signals observed in the $^{31}\text{P}\{-^1\text{H}\}$ NMR correspond to polynuclear non-hydrido species. These are not catalytically active species and their concentration is probably not significant in real dilute catalytic solutions. However, their signals often overwhelm the ^{31}P NMR spectra, which are run in relatively concentrated solutions. By increasing the partial pressure of H_2 , the relative intensity of those signals can be reduced with respect to that of the hydrido species. One of these species shows a broad doublet centred at $\delta 45.3$ ($J_{\text{Rh-P}} = 130$ Hz) at room temperature. At 65°C the signal splits into two doublets ($\delta 46.3$, $J_{\text{Rh-P}} = 147$ Hz; $\delta 42.1$, $J_{\text{Rh-P}} = 129$ Hz) with a fine structure reminiscent of a pseudotriplet. The signal could correspond to the species **11** in Scheme 4. For the homologous complex with dppe, James *et al.*¹⁹ reported a doublet centred at $\delta 38.1$ ($J_{\text{Rh-P}} = 138$ Hz). Furthermore, analogous complexes with dppp and with bdpp show pseudodoublets at room temperature, which also split into two set of doublets, but in these cases on lowering the temperature.^{9,19} The last $^{31}\text{P}\{-^1\text{H}\}$ NMR signal is an intense multiplet centred at $\delta 25.4$. The chemical shift is in the region characteristic of the binuclear complexes formed by PEtPh_2 . It resolves into two clean doublets ($\delta 23.6$, $J_{\text{Rh-P}} = 139$ Hz; $\delta 25.3$, $J_{\text{Rh-P}} = 119$ Hz) when the temperature is raised to 65°C . Thus, the signal should correspond to a binuclear species related to **11**, but where ligand **I** is co-ordinated in a monodentate or bridging mode. Nevertheless, the precise stoichiometry of the complex remains unclear.

In conclusion, although ligand **I** or its derivatives readily form chelates in square-planar complexes,²² rhodium five-co-ordinated species where **I** is acting in bridging or monodentate mode are observed under hydroformylation conditions. To our knowledge, the tendency of **I** to act as a monodentate ligand instead of a five-membered chelate has not previously been noticed. An early precedent of a 1,2-diphosphine acting both as chelate and as a bridging ligand was found in the reaction of $[\text{Ni}(\text{CO})_4]$ with dppe related ligands, which was reported to form species $[\{\text{Ni}(\text{CO})_2(\text{PP})\}_n]$ ($n = 1$ or 2).²³ Other examples of bridging 1,2-diphosphines, such as $\text{Ph}_2\text{P}(\text{CH}_2)_2\text{PPhMe}$ or $\text{Me}_2\text{P}(\text{CH}_2)_2\text{PMe}_2$, have also been reported.²⁴

Table 5 Natural and dynamic bite angles, flexibility ranges, and chelation energies obtained by molecular mechanics (see text). Crystallographic bite angles for complexes $[\text{Rh}(\text{L})(\text{cod})\text{X}]$ (L = diphosphine; X = non-co-ordinating anion) are also included

Ligand	Bite angle/ $^\circ$			Flexibility range/ $^\circ$	Chelation energy/ kcal mol^{-1}
	Natural	X-Ray ²¹	Dynamic		
I	84.0	84.6	84.3	74–94	11.6
bdpp	85.5	88.4	96.4	73–101	5.6
chiraphos	80.5	83.8	81.6	70–91	6.7

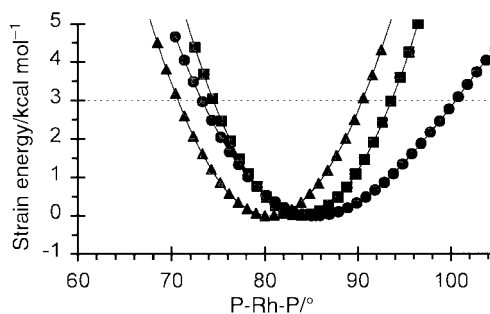


Fig. 5 Calculated excess strain energy of rhodium chelates of ligands **I** (■), bdpp (●) and chiraphos (▲) as a function of P–Rh–P angle. The horizontal line is drawn 3 kcal mol^{-1} above the energy minimum.

Furthermore, related to this result, Brown and Kent¹⁵ reported a higher stability for $[\text{RhH}(\text{CO})_2(\text{PP})]$ complexes with the six-membered chelate of dppp, than with the five-membered dppe. It could be speculated that 1,2-diphosphines have some tendency to form five-co-ordinated rhodium carbonyl species, where they act as monodentate ligands. This tendency should be more marked in the case of ligand **I**, because of the rigidity imposed by the cyclic backbone. The presence of open chelates in the catalytic mixtures could be one of the reasons for the poor results achieved with homochiral 1,2-diphosphines in rhodium asymmetric hydroformylation. It should be noted that many of these ligands are highly enantioselective in other processes, which involve square-planar or octahedral intermediates. For instance, rhodium complexes of ligand **I** yield e.e.s of around 90% both in acrylic acid hydrogenation²⁵ and in the hydrogen transfer from formate to the same substrates.²⁶

Molecular mechanics calculations

Molecular mechanics calculations were carried out on the $\text{Rh}(\text{PP})$ fragments (PP = **I**, chiraphos or bdpp) in order to compare their natural bite angles, chelate flexibilities and chelating tendencies. Data are collected in Table 5. The calculated natural bite angles are in agreement with the crystallographic P–Rh–P angles for structures $[\text{Rh}(\text{PP})(\text{cod})\text{X}]$ (cod = 1,5-cyclooctadiene; X = non-co-ordinating anion)²² within 3° . The overall concordance of the bond distances and the rest of the angles is also quite satisfactory. As expected, the six-membered chelating ligand bdpp shows a larger natural bite angle (85.5°) than chiraphos (80.5°). Although ligand **I** forms a five-membered ring, its natural bite angle (84.0°) is very close to that of bdpp, because the pyrrolidinic ring forces the two PPh₂ fragments to move away. However, these differences could hardly account for the disparate catalytic behaviour shown by these ligands. It is also worth noting that, since the bite angle model does not take into account the orientation of the phosphorus lone pairs, it does not reflect the low tendency of ligand **I** to form chelates.

Two approaches were used to measure the flexibility of the chelate rings. First, potential energy diagrams^{16,27} were calculated. The results are shown in Fig. 5. Owing to its structural

rigidity, ligand **I** presents the narrowest bite angle range accessible by 3 kcal of strain energy. On the other hand, the chelate of **bdpp** shows the widest range, which reflects its higher structural flexibility, compared with that of **I** or **chiraphos**. The last two show a symmetric potential energy curve around their natural bite angle, in contrast with the curve of **bdpp**, which shows a lower gradient at angle values above equilibrium. Thus, chelation angles higher than its natural bite angle are accessible for the **bdpp** ligand with a low cost in energy. This fact was corroborated by dynamically calculating averaged bite angles for these ligands at 400 K. This temperature, slightly above reaction conditions, was chosen to emphasize the observed patterns. Ligand **I** shows an average dynamic angle nearly identical to the natural bite angle. The dynamic angle for **chiraphos** is slightly higher than its natural bite angle, and it matches the crystallographic value. Finally, **bdpp** shows a dynamic angle of 96.4°, which is significantly higher than the static angle (85.5°). This result again indicates that, although ligand **I** and **bdpp** show similar static natural bite angles, the latter can reach relatively wide chelating angles, which are not accessible by ligand **I**. A recent report¹⁴ suggests that the geometry of the four-co-ordinated species $\text{Rh}(\text{CO})(\text{PP})$ is crucial in determining the selectivity of rhodium–diphosphane catalysts. In this context, the possibility of **bdpp** easily to open its bite angle up to 100°, a value not accessible for ligand **I** or for **chiraphos**, could be the origin of the higher stereoselectivity showed by the catalytic species formed with **bdpp**.

Since the catalytic and NMR experiments show some evidence for a bridging bidentate co-ordination of ligand **I**, we have also evaluated the chelating tendency of this ligand, and compared it with those of ligands **bdpp** and **chiraphos**. Thus, we calculated the differences in strain energies between the ligands in their most stable chelate and monodentate conformations, as described in the Experimental section. The results show that ligand **I** has an energy increase upon chelation (12 kcal mol⁻¹) of about twice that of **bdpp** or **chiraphos**. This again reflects a low tendency of ligand **I** to act as chelating ligand.

Conclusion

In the hydroformylation of styrene the rhodium catalytic system containing ligand **I** shows a different behaviour to that of related ligands **chiraphos** or **bdpp**. The NMR experiments provided evidence for the presence of rhodium five-co-ordinated species where ligand **I** is co-ordinated in both bridging and chelating modes. Molecular mechanics calculations indicate a lower tendency of ligand **I** to form a chelate, compared with **bdpp** or **chiraphos**. Thus, the similar regioselectivity observed for rhodium catalytic systems with ligand **I** and with $\text{P}(\text{EtPh}_2)_3$, and the nearly null enantioselective discrimination of the former could be related with the presence of a catalytically active species in which the diphosphine co-ordinates each metal in a monodentate mode.

Experimental

Solvents were purified by standard procedures. Ligand **I** and $[\text{Rh}_2(\mu\text{-OMe})_2(\text{cod})_2]$ were synthesized by modified procedures of those described in the literature.^{28,29} The product **I** was compared with a sample kindly supplied by Degussa Ibérica S.A. All air sensitive materials were handled using standard vacuum and inert atmosphere techniques.

Apparatus

The hydroformylation reactions were performed in an 80 ml stainless steel home-made autoclave. The solution was contained in a glass inlet. The inside autoclave cap was Teflon covered to avoid direct contact of the solution with the steel.

The solution was magnetically stirred and the temperature controlled by a water-bath circulating through an external jacket. The pressure of the autoclave was kept constant by means of a regulator, connected to a syn-gas reservoir. The evolution of the reaction was monitored by the drop in the reservoir pressure.

Conversions and regioselectivity were determined by gas chromatography in a Hewlett-Packard G1800A, equipped with a capillary HP5 column (30 m × 0.25 mm). Enantiomeric excesses were measured with a Konik-300C gas chromatograph equipped with β -cyclodextrin capillary column, Supelco β -Dex-120, 30 m × 0.25 mm, after reduction of the aldehydes to the corresponding alcohols with LiAlH_4 .

The ¹H, ¹³C and ³¹P NMR spectra were registered on Bruker 250 MHz or Varian 300 MHz instruments and they were referenced in the usual way. High-pressure NMR experiments were carried out in a 10 mm diameter sapphire tube with a titanium cap. The spectra were simulated with gNMR 4.0.³⁰

Catalytic hydroformylation of styrene: general procedure

The complex $[\text{Rh}_2(\mu\text{-OMe})_2(\text{cod})_2]$, 6 mg (0.0125 mmol), and the desired amount of the diphosphine **I** were placed in a Schlenk flask. The flask was purged, and 15 ml of toluene plus 1.2 ml of styrene (10 mmol) were injected. The solution was purged and transferred to the evacuated autoclave, which was pressurized up to about half of the working pressure and heated to the desired temperature. When thermal equilibrium was reached the pressure was adjusted and stirring initiated. One ml aliquots were removed *via* the liquid sample valve to measure the selectivity as the reaction proceeded. Conversion and regioselectivity in these samples and in the final solution were directly analysed by GC. Samples were immediately reduced with a suspension of LiAlH_4 in THF. The resulting alcohols were analysed in the chiral GC column to determine the enantiomeric excess.

Hydroformylation reaction using diphosphine **II** and triethyl orthoformate

The procedure described above was used, except that toluene was replaced by triethyl orthoformate, and diphosphine **II** was used instead of **I**. Conversion and regioselectivity of produced ethyl acetals were directly determined by GC. A sample of the intermediate or final solution was diluted with 5 ml of diethyl ether, and stirred for 10 min with 5 ml of 1 M aqueous HCl. The mixture was extracted with CH_2Cl_2 . One part of the solution was used to corroborate the conversion and regioselectivity in the formation of aldehydes, and the rest was immediately reduced as described above to determine the enantiomeric excess.

Molecular mechanics

The molecular mechanics calculations were carried out using the TINKER package,³¹ with the included MM3 (96) force field. Parameters involving rhodium were taken from Casey and Whiteker,²⁷ except for the Rh–P bond length, for which a value of 2.315 Å was used.³² For the rest of the ring parameters not defined in MM3 those corresponding to a straight chain were used. The energy optimization was carried out with the TINKER program MINIMIZE, until the rms dropped below 0.01 kcal mol⁻¹. The SNIFFER and DYNAMIC modules were also used to locate the most stable conformers.

Natural bite angles and strain energies for deviation from the corresponding equilibrium values were calculated as previously reported.^{16,27} In the latter, when specific values of the bite angle were imposed through a penalty function, the angle deviation did not exceed 0.5°. The dynamic bite angle was calculated with the DYNAMIC module of TINKER. The optimized geometry for each chelate was used as starting point. The temperature was set at 400 K. The bite angle was recorded each 10 fs, and an

average of the first 100 values was assumed to be the dynamic bite angle. A larger number of values did not affect the average.

To quantify the tendency of the ligands to act in a monodentate fashion, the fragments Rh(PP,monodentate) were optimized. The metal atom was then removed from this, and from the optimized chelate fragment, and the strain energy of both pure ligand conformations calculated. The difference between the two values was taken as a measure of the tendency of each ligand to open one side arm.

Since the TINKER package has not been used before for this type of compound some tests were conducted to validate the results. First, the ability to determine natural bite angles close to 90°, such as that of dppe, or largely exceeding this value (DBFphos, 1,8-bis(diphenylphosphino)dibenzofuran), and the intervals of the angles corresponding to strain energies not exceeding 3 kcal mol⁻¹ were reproduced in satisfactory agreement with previous determinations.^{27,32} Furthermore, the optimized structure for ligand **I** was obtained with a PM3 semi-empirical calculation by resorting to the GAMESS package.³³ The geometrical parameters thus determined are also in close agreement with the molecular mechanic calculations.

Acknowledgements

We are grateful to Ministerio de Educación y Ciencia and Direcció General de Recerca (project QFN95-725-C03) and Portugal-Spain Cooperative Action (HP97-0059) for financial support. We would also like to thank Junta Nacional de Investigação Científica e Tecnológica for a visiting grant for M. M. P. (Praxis XXI-BDP9966). The authors are indebted to A. Masdeu-Bultó and R. Guerrero (Universitat Rovira i Virgili, Tarragona) for their help in the use of HPNMR facility, and to Degussa Iberica SA for a kind gift of ligand **I**.

References

- 1 G. Consiglio, in *Catalytic Asymmetric Synthesis*, ed. I. Ojima, VCH, Weinheim, 1993, pp. 273–302.
- 2 F. Agbossou, J. F. Carpentier and A. Mortreux, *Chem. Rev.*, 1995, **95**, 2485; S. Gladiali, J. C. Bayón and C. Claver, *Tetrahedron: Asymmetry*, 1995, **6**, 1453.
- 3 N. Sakai, S. Mano, K. Nozaki and H. Takaya, *J. Am. Chem. Soc.*, 1993, **115**, 7033.
- 4 G. J. H. Buisman, E. J. Vos, P. C. J. Kamer and P. W. N. M. van Leeuwen, *J. Chem. Soc., Dalton Trans.*, 1995, 409; J. E. Babin and G. T. Whiteker, *P.C.T. Int. Appl.*, WO 93/03830, 1992.
- 5 T. V. RajanBabu and T. A. Ayers, *Tetrahedron Lett.*, 1994, **35**, 4295.
- 6 N. Sakai, K. Nozaki and H. Takaya, *J. Chem. Soc., Chem. Commun.*, 1994, 395; T. Nanno, N. Sakai, K. Nozaki and H. Takaya, *Tetrahedron: Asymmetry*, 1995, **6**, 2583; T. Horiuchi, T. Ohta, E. Shirakawa, K. Nozaki and H. Takaya, *J. Org. Chem.*, 1997, **62**, 4285.

- 7 P. W. N. M. van Leeuwen, G. J. H. Buisman, A. van Rooy and P. C. J. Kamer, *Recl. Trav. Chim. Pays-Bas*, 1994, **113**, 61; K. Nozaki, N. Sakai, T. Nanno, T. Higashijima, S. Mano, T. Horiuchi and H. Takaya, *J. Am. Chem. Soc.*, 1997, **119**, 4413.
- 8 A. M. Masdeu, A. Orejón, A. Castellanos, S. Castellón and C. Claver, *Tetrahedron: Asymmetry*, 1996, **7**, 1829.
- 9 A. Castellanos-Páez, S. Castellón, C. Claver, P. W. N. M. van Leeuwen and W. G. J. de Lange, *Organometallics*, 1998, **17**, 2543.
- 10 M. Diéguez, M. M. Pereira, A. M. Masdeu-Bultó, C. Claver and J. C. Bayón, *J. Mol. Catal.*, 1999, **143**, 111.
- 11 U. Nagel, E. Kinzel, J. Andrade and G. Prescher, *Chem. Ber.*, 1986, **119**, 3326.
- 12 G. Parrinello and J. K. Stille, *J. Am. Chem. Soc.*, 1987, **109**, 7122.
- 13 E. Fernández and S. Castellón, *Tetrahedron Lett.*, 1994, **35**, 2361.
- 14 L. A. van der Veen, M. D. K. Boele, F. R. Bregman, P. C. J. Kamer, P. W. N. M. van Leeuwen, K. Goubitz, J. Fraanje, H. Schenk and C. Bo, *J. Am. Chem. Soc.*, 1998, **120**, 11616.
- 15 J. M. Brown and A. G. Kent, *J. Chem. Soc., Perkin Trans. 2*, 1987, 1597.
- 16 C. P. Casey, G. T. Whiteker, M. G. Melville, L. M. Petrovich, J. A. Gavney Jr. and D. R. Powell, *J. Am. Chem. Soc.*, 1992, **114**, 5535.
- 17 O. R. Hughes and D. A. Young, *J. Am. Chem. Soc.*, 1981, **103**, 6636.
- 18 P. E. Garrou, *Chem. Rev.*, 1981, **81**, 229.
- 19 B. R. James, D. Mahajan, S. J. Rettig and G. M. Williams, *Organometallics*, 1983, **2**, 1452.
- 20 B. R. James and D. Mahajan, *Can. J. Chem.*, 1979, **57**, 180.
- 21 Z. Freixa and J. C. Bayón, unpublished work.
- 22 J. Bakos, I. Toth, B. Heil, G. Szalontai, L. Parkanyi and V. Fulop, *J. Organomet. Chem.*, 1989, **370**, 263; R. G. Ball and N. C. Payne, *Inorg. Chem.*, 1977, **16**, 1187; U. Nagel and B. Rieger, *Chem. Ber.*, 1988, **121**, 1123.
- 23 L. S. Meriwether and J. R. Leto, *J. Am. Chem. Soc.*, 1961, **53**, 3192.
- 24 S. O. Grim, J. del Gaudio, R. P. Molenda, C. A. Tolman and J. P. Jesson, *J. Am. Chem. Soc.*, 1974, **96**, 3416; J. A. Connor, G. K. McEwen and C. J. Rix, *J. Chem. Soc., Dalton Trans.*, 1974, 589; K. R. Pörschke and R. Mynott, *Z. Naturforsch., Teil B*, 1984, **39**, 1565; J. Chatt and F. H. Hart, *J. Chem. Soc.*, 1960, 1378.
- 25 U. Nagel, *Angew. Chem., Int. Ed. Engl.*, 1984, **23**, 435.
- 26 A. M. d'A. Rocha Gonsalves, J. C. Bayón, M. M. Pereira, M. E. S. Serra and J. P. R. Pereira, *J. Organomet. Chem.*, 1998, **553**, 199.
- 27 C. P. Casey and G. T. Whiteker, *Isr. J. Chem.*, 1990, **30**, 299.
- 28 M. E. S. Serra, Ph.D. Thesis, Univerdidade de Coimbra, 1998.
- 29 R. Usón, L. A. Oro and J. Cabeza, *Inorg. Synth.*, 1985, **23**, 126.
- 30 P. H. M. Budzelaar, gNMR, Ivory Soft, Chervell Scientific Publishers, Oxford, 1998.
- 31 Y. Kong and J. W. Ponder, *J. Chem. Phys.*, 1997, **107**, 481; M. J. Dudek and J. W. Ponder, *J. Comput. Chem.*, 1995, **16**, 791; C. E. Kundrot, *J. Comput. Chem.*, 1991, **12**, 402; J. W. Ponder and F. M. Richards, *J. Comput. Chem.*, 1987, **8**, 1016.
- 32 M. Kranenburg, Y. E. M. van der Burgt, P. C. J. Kamer and P. W. N. M. van Leeuwen, *Organometallics*, 1995, **14**, 3081.
- 33 M. W. Schmidt, K. K. Baldrige and J. A. Boatz, *J. Comput. Chem.*, 1993, **14**, 1347.

Paper 9/04019F